EXCESS NOISE IN $Pb_{1-x}Sn_xSe$ SEMICONDUCTOR LASERS

Charles N. Harward
Department of Physics
Old Dominion University

and

Barry D. Sidney
NASA Langley Research Center

INTRODUCTION

Tunable Diode Lasers (TDL) have been used for several years as ultra narrow band (<30 MHz) sources for ultra high resolution spectroscopy of many different infrared absorbing gases. Interest in the TDL has been increasing in recent years due to their possible use in different types of spectroscopic systems, i.e., Laser Absorption Spectrometer (LAS) and Laser Heterodyne Spectrometer (LHS). These systems all have the common goal of making remote or in situ measurements of one or several atmospheric gases and use the TDL as a spectroscopic source. Because of the interest in high detection sensitivities, the noise characteristics of the TDL have been studied for frequencies less than 20 kHz (refs. 1 to 3). For heterodyne applications, the high frequency (>1 MHz) characteristics are also important. Therefore, we have studied the high frequency noise characteristics of the TDL as a part of a full TDL characterization program which has been implemented at Langley Research Center for the improvement of the TDL as a local oscillator in the LHS system. In this study which involved the characterization of TDL's from two commercial sources (Laser Analytics and New England Research Center) and one private source (General Motors Research Laboratory), it has been observed that all the devices showed similar high frequency noise characteristics even though they were all constructed using different techniques. We will now report these common high frequency noise characteristics.

EXPERIMENTAL DETAILS

The TDL noise characteristics facility is shown in figure 1. The TDL is mounted in a commercial closed cycle cooler which has been modified to minimize frequency fluctuations which are induced during the cooling cycle. Radiation is coupled through a wedged AR coated ZnSe window to a 37 mm f/1 Ge lens which collimates the TDL emission. This collimated beam passes either to a high speed HgCdTe detector (IF bandwidth ≈ 2 GHz) or to a monochromator. The monochromator was used to investigate the spectral characteristics of the TDL output. The high speed detector was used to measure the high frequency noise characteristics of the TDL output. The detector high frequency output was amplified by two cascaded IF amplifiers which were followed by a square law detector used to

rectify and integrate the IF output. The low frequency portion of the detector output and the integrated IF were monitored on a dual channel oscilloscope. At times, the frequency distribution of the IF was displayed on a spectrum analyzer.

The high frequency noise present in the TDL output for the numerous devices studied can be categorized according to frequency characteristics. Figure 2(a) shows a typical example of what we have categorized as low frequency noise (<100 MHz). The spectrum analyzer was set on 10 MHz/div with a 300 kHz resolution bandwidth and 10 dB/div. The zero frequency is located at the start of the left to right scan. For this particular spectrum, the noise drops to the constant baseline value in the first 30 MHz. In other cases, the noise extended out to 100 MHz. This type of noise can be caused either by a small amount of optical feedback or by physical phenomena intrinsic to the semiconductor laser itself. In the example represented in figure 2(a) the noise is associated with low frequency switching between laser modes (or sets of modes) at a particular current and temperature.

The second category of noise is the type which contains one or several narrow band spikes. In the case of several spikes, the spikes sometimes form a harmonic sequence (ref. 4). This type of structure is shown in figure 2(b). The total frequency was 1.2 GHz. The noise shown here is sometimes associated with the frequency of intensity self-pulsations (refs. 5 to 8) and is called self-pulsation noise. The harmonics appearing in the noise spectra may come from the waveform distortion in the pulsing light output (ref. 9). This category of noise is also associated with a heterodyne beating between closely spaced transverse modes. Harward and Hoell (ref. 10) have reported this type of harmonic structure for Pb-salt lasers with optical feedback while Broom and others (refs. 11 to 14) have shown this to be true for GaAs semiconductor lasers. Figure 2(c) shows the harmonic structure induced by optical feedback. The spacing between the peaks is commensurate with the spacing between the feedback element and the TDL.

The case of a single narrow frequency spike is shown in figure 2(d). This type of structure has been the subject of experimental and theoretical investigations in GaAs (refs. 15 to 19). The theoretical treatment of McCumber (ref. 15) for fluctuations in multimode laser oscillators was based on simple rate equations. The intrinsic quantum fluctuations drive the coupled electron and photon distributions at a characteristic resonance spiking frequency. This type of noise is called resonant shot noise.

The last category of noise structure has a broadband nature. This is shown in figure 2(e) for a 0 to 1.2 GHz spectrum. The noise structure is seen to rise above the no-noise baseline (bottom trace) in a more or less uniform manner. The broadband structure may be associated with the "low" frequency tail of a resonance where the spiking frequency is greater than the maximum frequency of the spectrum analyzer. This type of tail has also been seen in GaAs (refs. 13 and 20).

The next figures show the spatial dependence of both the direct detected power and the IF integrated noise. The bottom and top trace in each of the photographs in figures 3(a), (b), and (c) are, respectively, the TDL direct

detected power and the IF integrated noise present in the TDL output. For these measurements an etalon is inserted into the beam path and scanned through one free spectral range. Each of the figures 3(a), (b), and (c) are for different spatial positions in the TDL image. Each spatial position produces a different modal distribution of both the TDL power and the IF noise. The differential translation between each measurement was about 25 μm. The highest power TDL mode does not have the highest IF noise. In fact, numerous cases have been observed in which a very small mode has a very large amount of noise. Each of the figures 3(a), (b), and (c) were taken at the same temperature and current conditions on the TDL. The observed spatial dependence of the mode and noise mode structure has been observed in GaAs and has been attributed to different lasing filaments in the laser junction (refs. 18 and 21). Due to the aberrations in the present optical system, the individual lasing filaments cannot be optically separated. Their presence is substantiated by the spatial dependence of the TDL modes.

Figure 3(d) shows the output for the same spatial position as in figure 3(c), but with the etalon removed. All TDL modes present in figure 3(c) are present on the detector simultaneously in figure 3(d). The bottom trace, which was AC coupled, shows a variation not observable in the previous cases because the total power level is much higher. The variation was caused by mechanical vibrations in the closed cycle cooler. The upper trace, which was DC coupled, shows that the noise level is much reduced (in this case to zero) when all of the TDL modes are incident on the detector. The figure shows that the high frequency noise of a single mode which is caused by high frequency intensity fluctuations, is, for a multimode laser, higher than fluctuations of the total output. This result occurs because the strong negative correlations between the single, coherently oscillating mode and the nonlasing modes act to reduce the total noise output. This result, too, has been observed in GaAs semiconductor lasers (refs. 20 and 22). Both of these references have reported single mode noise power levels 30 dB higher than the noise power for all modes. The noise in this case has been given the name partition noise and is associated with multimode operation. The decrease in noise when multimodes are incident on a detector compared to the noise in a single mode is called noise amplitude stabilization.

In the previous set of figures, the spatial dependence of TDL mode structure was demonstrated along with the phenomena of noise amplitude stabilization. In figure 4, parts (a), (c), and (e) also show the spatial dependence of the mode structure and the IF noise while parts (b), (d), and (f) show the spatial dependence of the noise amplitude stabilization. Figures 4(a), (c), and (e) were obtained in the same manner as figures 3(a), (b), and (c) (for a different current and temperature). The variation in the individual mode power with spatial position as well as variation in the IF integrated noise is again observed. Figures 4(b), (d), and (f) were obtained by synchronizing the oscilloscope to a mechanical chopper which replaced the scanning etalon at each position. (The chopper was used to determine the noise baseline with no TDL radiation on the detector.) These figures were obtained at the same positions as figures 4(a), (c), and (e), respectively. Figure 4(b) shows only a slight amount of noise when all modes are incident on the detector even though the individual modes appear to be much noisier. At this position, the noise is again amplitude stabilized as in figure 3(d). As the detector is translated

across the TDL image to obtain figures 4(d) and (f), the amount of IF noise variation is much larger than the variation in the direct detected power, indicating a spatial dependence of the noise amplitude stabilization.

Figures 5(a), (b), and (c) show the spatial dependence of the TDL modes and the IF noise in these modes for a different current and temperature than was used in the previous figure. These figures were also obtained by moving the high speed detector to different positions in the image of the TDL. The difference in the TDL modes and the IF noise generated by these modes is evident for the three spatial positions. These results are similar to those shown in figures 3(a), (b), and (c), and 4(a), (b), and (c), except that two sets of longitudinal modes have been identified in the direct detected TDL mode spectra. These are indicated by the two sets of equally spaced lines at the top of each figure. The breaking up of the TDL output into two groups of longitudinal modes is suggested by the appearance of the IF integrated noise in figure 4(a) which is dominated by the noise generated by one set of longitudinal modes. The appearance of two sets of longitudinal modes is a common occurrence in GaAs lasers and has been attributed to different lasing filaments (refs. 21, 23, and 24). Each filament may act as an independent laser with its own family of modes. The different characteristic wavelengths are due to material inhomogeneities. Optical coupling between filaments was reported by Deutsch and Hatz (ref. 25) as well as uncoupled filaments by Guekos and Strutt (ref. 21).

Figures 6 and 7 indicate that the interaction between lasing filaments is involved in the appearance of excess noise in the laser modes. The curves in figures 6(a) to (e) show monochromator spectral mode scans of the TDL output from 9.35 to 9.47 μm for different TDL injection currents. The current in scan (a) was 1.337 amps and in each succeeding scan, the current was increased by 1.0 mA. Scans (a) to (c) show little variation in the mode structure. The TDL output was made up mainly of the modes labeled 1, 4, 5, and 7. At $I = 1.340$ amps, modes 2, 3, and 6 appear. The relative spacing of all the modes indicate modes 2, 3, and 6 belong to one lasing filament while 1, 4, 5, and 7 belong to another. Table I shows how the power in the individual modes changes with current. The total power in the modes remains relatively constant, with the power decrease in modes $1 + 4 + 5 + 7$ matched by an increase in modes $2 + 3 + 6$. The large change in power in the modes occurs at $I = 1.340$ amps where modes 2, 3, and 6 appear. The appearance of these modes coincides with the occurrence of broadband excess noise in all the TDL modes. Thus, the noise is associated with the appearance of the second filament and is probably due to an interaction between the filaments either in the TDL, caused by coupling of the filaments, or on the detector, caused by a beating between the filaments. The first case is the more likely since the noise was observed to be broadband rather than of the spiking resonance type, and the relative separation of the individual modes gives rise to beat frequencies which are higher than our system bandwidth.

Figure 6 shows that the appearance of a new filament, as indicated by the appearance of new laser modes, coincided with the onset of excess noise, thus implying that the onset of filamentary operation was responsible for excess noise. The next figure shows that filamentary operation, per se, does not necessarily give rise to excess noise. Figure 7 shows the same type mode scan as in figure 6. In figures (a) to (l), the current is changed from 1.7895 to

1.8005 amps in 1 mA steps. The spacing between modes indicates modes 1, 3, and 5 belong to one set of axial modes associated with one filament while modes 2, 4, and 6 belong to another set and, thus, another filament. The excess noise is not present in the TDL output in mode scans (a) to (e). Starting with scan (f) and continuing, the TDL output shows excess noise. Examination of table II shows that while changes occur in the individual modes, the relative power in each set of modes, as well as the total power, remains relatively constant. The exact cause of the noise is not known. One possible explanation is that, initially, the two filaments were sufficiently spatially separated so that they were uncoupled and noninteracting. The current increase from 1.7935 to 1.7945 amps may then have caused a slight spatial shift of the filaments sufficient to cause interaction between them with the consequent production of excess noise. Both uncoupled and coupled filaments have been observed in GaAs (refs. 21 and 25).

Figure 8(a) shows a TDL operating multimode with no excess noise in individual modes. The bottom trace of the figure shows the direct detected TDL mode structure obtained with the scanning etalon. The top trace shows no excess noise in the integrated IF for the individual TDL modes. Moving the detector about in the TDL image did not show a change in the mode structure as has been observed in previous figures, indicating only one lasing filament. Thus, this is one more indication that excess noise may in some cases be caused by an interaction between lasing filaments. Figure 8(b) shows the output of the TDL which is also quiet when all the modes are incident on the detector. In this figure, the scanning etalon was replaced by a mechanical chopper as in some of the previous figures. Since the individual modes are quiet, any one of these modes may be optically isolated and used as a spectroscopic source in a high speed detection system.

CONCLUDING REMARKS

In summary, we have shown that excess noise generated by Pb-salt lasers can be classified according to high frequency content and we have indicated a possible explanation for each noise category. We have shown the spatial dependence of the TDL modes and the IF noise associated with these modes which indicated that the semiconductor lasers tested sometimes emit simultaneously in two or more lasing filaments. Results presented show that multiple filaments are at times involved in the mechanism which generates excess noise although the mere presence of multiple filaments does not guarantee that excess noise will be present.

Throughout the results presented, we have shown the similarity between the $Pb_{1-x}Sn_xSe$ semiconductor lasers and the results of other workers on GaAs semiconductor lasers. Although these two materials are different and emit radiation at different wavelength regions, the similarities are such that the techniques used to control the excess noise in the GaAs semiconductor lasers may also work on the Pb-salt lasers.

REFERENCES

1. Savage, M.; Augeri, R.; and Peyton, B. J.: Application of Tunable Diode Lasers to Infrared Heterodyne Spectroscopy. Second Conference on Lasers and Applications (Orlando, Fla.), Dec. 17-21, 1979.

2. Eng, R. S.; Mantz, A. W.; and Todd, T. R.: Improved Sensitivity of Tunable-Diode Laser Open Path Trace Gas Monitoring System. Appl. Opt., 18, 3438, 1979.

3. Eng, R. S.; Mantz, A. W.; and Todd, T. R.: Low Frequency Noise Characteristics of Pb-Salt Semiconductor Lasers. Appl. Opt., 18, 1088, 1979.

4. Paoli, T. L.; and Ripper, J. E.: Coupled Longitudinal Mode Pulsing in Semiconductor Lasers. Phy. Rev. Lett., 22, 1085, 1969.

5. Paoli, T.; and Ripper, J.: Observation of Intrinsic Quantum Fluctuations in Semiconductor Lasers. IEEE J. Quant. Elect., QE-6, 325, 1970.

6. Bogatov, A. P.; Eliseev, P. G.; Logginov, A. S.; Manko, M. A.; and Senatorov, K.: Study of the Single-Mode Injection Laser. IEEE J. Quant. Elect., QE-9, 392, 1973.

7. Eliseev, P. G.; and Shuikin, N. N.: Single Mode and Single Frequency Injection Lasers. Sov. J. Quant. Electron, 3, 181, 1973.

8. Bachert, H.; Eliseev, P.; Maneo, V.; Stremov, S.; Raab; and Thay, C.: Multimode Operation and Mode-Locking Effect in Injection Lasers. IEEE J. Quant. Elect., QE-11, 507, 1975.

9. Kobayashi, T.; Takaneshi, Y.; and Fusukana, Y.: Reduction of Quantum Noise in Very Narrow Planer Stripe Lasers. Jap. J. of Appl. Phys., 17, 535, 1978.

10. Harward, C. N.; and Hoell, J. M.: Optical Feedback Effects on the Performance of $Pb_{1-x}Sn_xSe$ Semiconductor Lasers. Appl. Opt., 18, 3978, 1979.

11. Broom, R. F.: Self-Modulation at Gigahertz Frequencies of a Diode Laser Coupled to an External Cavity. Electronic Letters, 5, 571, 1969.

12. Broom, R. F.; Mohn, E.; Risch, C.; and Salathe, R.: Microwave Self-Modulation of a Diode Laser Coupled to an External Cavity. IEEE J. Quant. Elect., QE-6, 328, 1970.

13. Ho, P. T.; Glasser, L. A.; Ippen, E. P.; and Haus, H. A.: Picosecond Pulse Generation With a CW GaAlAs Laser. Appl. Phys. Lett., 33, 241, 1978.

14. Risch, C.; and Voumard, C.: Self-Pulsations in the Output Intensity and Spectrum of GaAs-AlGaAs CW Diode Lasers Coupled to a Frequency Selective External Optical Cavity. J. of Appl. Phys., 48, 2083, 1977.

15. McCumber, D. E.: Intensity Fluctuations in the Output of CW Laser Oscillators I. Phys. Rev., 141, 306, 1966.

16. Haug, H.; and Haken, H.: Theory of Noise in Semiconductor Laser Emission. Z. Physik, 204, 262, 1967.

17. Armstrong, J. A.; and Smith, A. W.: Intensity Fluctuations in GaAs Laser Emission. Phy. Rev., 140, A155, 1965.

18. Smith, A. W.; and Armstrong, J. A.: Intensity Noise in Multimode GaAs Laser Emission. IBM Res. Develop., 10, 225, 1966.

19. Guekos, G.; Jackel, H.; and Schmid, K. F.: Excess Noise in the Radiation From CW D. H. GaAlAs-Diode Lasers. Elect. Lett., 12, 64, 1975.

20. Jackel, H.; and Guekos, G.: High Frequency Intensity Noise Spectra of Axial Mode Groups in the Radiation From CW GaAlAs Diode Lasers. Opt. and Quan. Elect., 9, 233, 1977.

21. Guekos, G.; and Strutt, M. J.: Laser-Light Noise and Current Noise of GaAs CW Laser Diodes. IEEE J. Quant. Elect., QE-6, 423, 1970.

22. Ito, T.; Machida, S.; Nawata, K.; and Regami, T.: Intensity Fluctuations in Each Longitudinal Mode of a Multimode AlGaAs Laser. IEEE J. Quant. Elect., QE-13, 574, 1977.

23. Kingsley, T.; and Finner, G.: Stimulated Emission From P-N Junctions. Proc. 3rd International Congr., Quantum Electron. (Paris), Dunod, 1883, 1964.

24. Hatz, J.: Some Effects on Material Inhomogeneities on the Near Field Pattern of GaAs Diode Lasers. Phy. Status Solidi, 28, 233, 1968.

25. Deutsch, C.; and Hatz, J.: Observation of Mode Coupling in GaAs Lasers. J. Appl. Math. Phys. (ZAMP), 18, 599, 1967.

TABLE I.- PEAK HEIGHTS OF MEMBERS OF LONGITUDINAL MODE FAMILIES AT LASER CURRENTS FROM 1.337 TO 1.345 AMPS

Laser current, amps	Mode									
	1	2	3	4	5	6	7	2 + 3 + 6	1 + 4 + 5 + 7	Sum overall
1.337	15	0	0	19	12	0	12	0	58	58
1.338	16	0	0	19	12	0	12	0	59	59
1.339	17	0	0	19	11	0	12	0	59	59
1.340	16	1	1	19	8	0	13	2	56	58
1.341	7	7	16	8	3	4	12	27	30	57
1.342	6	8	18	6	3	4	12	30	27	57
1.343	6	8	19	5	2	5	13	32	26	58
1.344	5	8	20	5	2	5	13	33	25	58
1.345	5	8	21	4	2	5	13	34	24	58

TABLE II.- PEAK HEIGHTS OF MEMBERS OF LONGITUDINAL MODE FAMILIES AT LASER CURRENTS FROM 1.7895 TO 1.8005 AMPS

Laser current, amps	Mode								
	1	2	3	4	5	6	1 + 3 + 5	2 + 4 + 6	Sum overall
1.7895	5	8	9	14	10	8	24	30	54
1.7905	5	11	8	14	11	6	24	31	55
1.7915	4	13	8	13	12	3	24	29	53
1.7925	3	15	8	13	13	2	24	30	54
1.7935	3	17	8	13	13	1	24	31	55
1.7945	10	5	10	15	5	7	25	27	52
1.7955	11	4	11	18	5	8	27	30	57
1.7965	12	3	11	19	4	7	27	29	56
1.7975	12	3	11	20	4	7	27	30	57
1.7985	13	3	11	19	4	6	28	28	56
1.7995	15	2	11	20	3	5	29	27	56
1.8005	16	3	10	21	4	4	30	28	58

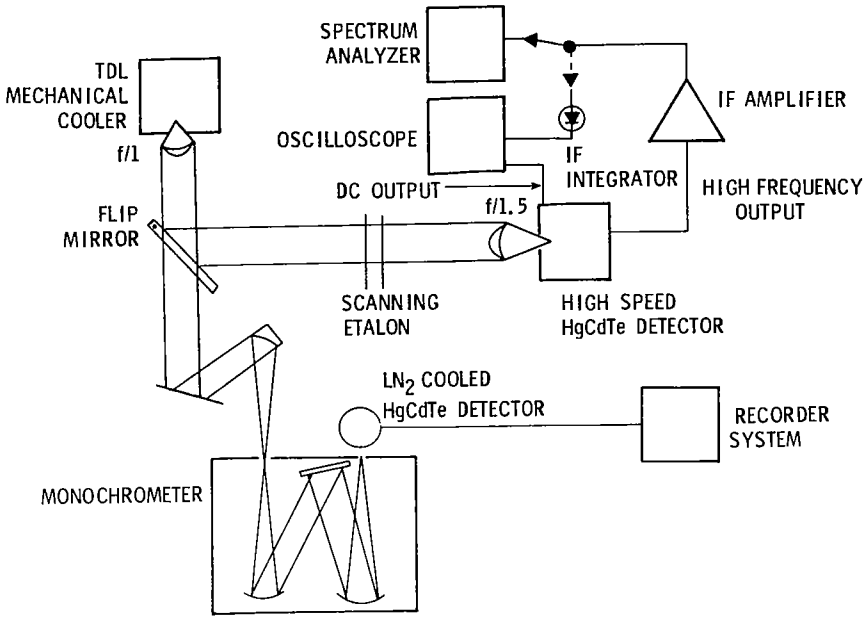

Figure 1.- TDL characterization facility.

(a) LOW FREQUENCY NOISE
(0-90 MHz)

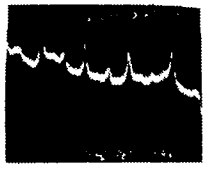

(b) HARMONIC SPIKING
RESONANCE
(0-1200 MHz)

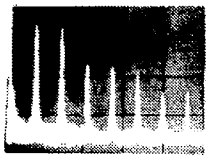

(c) OPTICAL FEEDBACK
INDUCED HARMONIC
RESONANCE
(0-500 MHz)

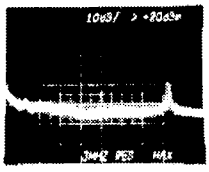

(d) SHOT NOISE INDUCED
SPIKING RESONANCE
OR
SELF-PULSATIONS
(0-1200 MHz)

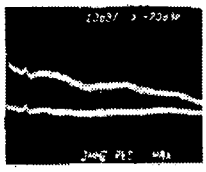

(e) BROADBAND NOISE
(0-1200 MHz)

Figure 2.- Categories of excess noise.

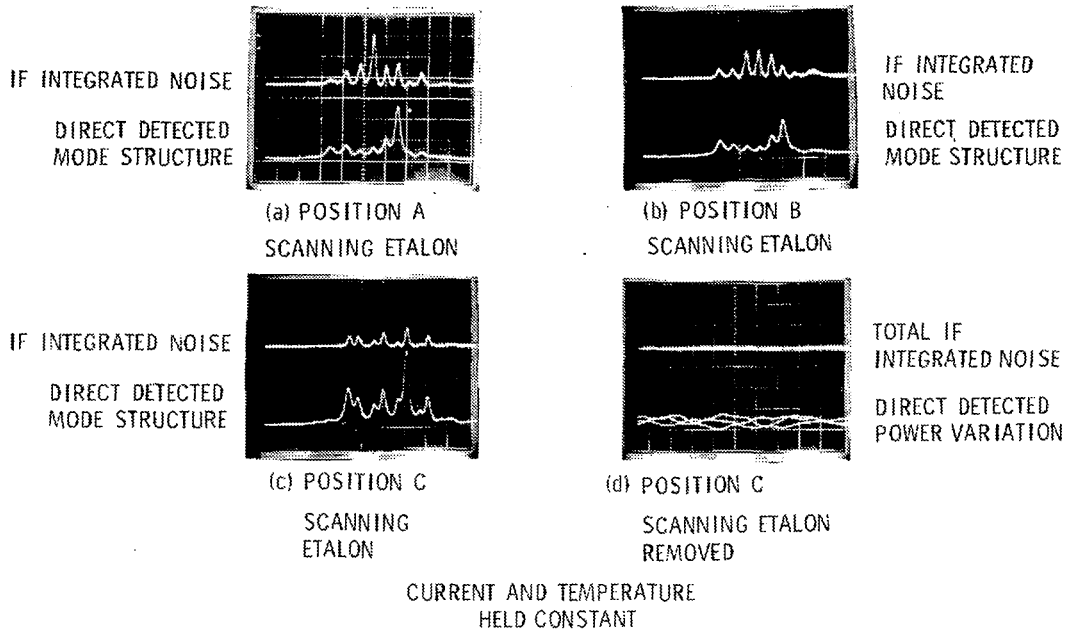

Figure 3.- Spatial dependence of TDL mode power and excess noise; noise amplitude stabilization.

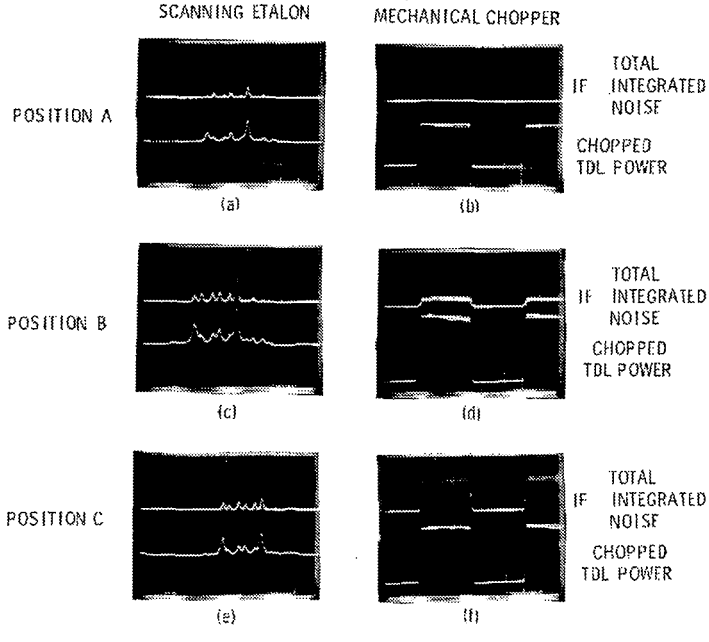

Figure 4.- Spatial dependence of TDL mode power, excess noise, and noise amplitude stabilization.

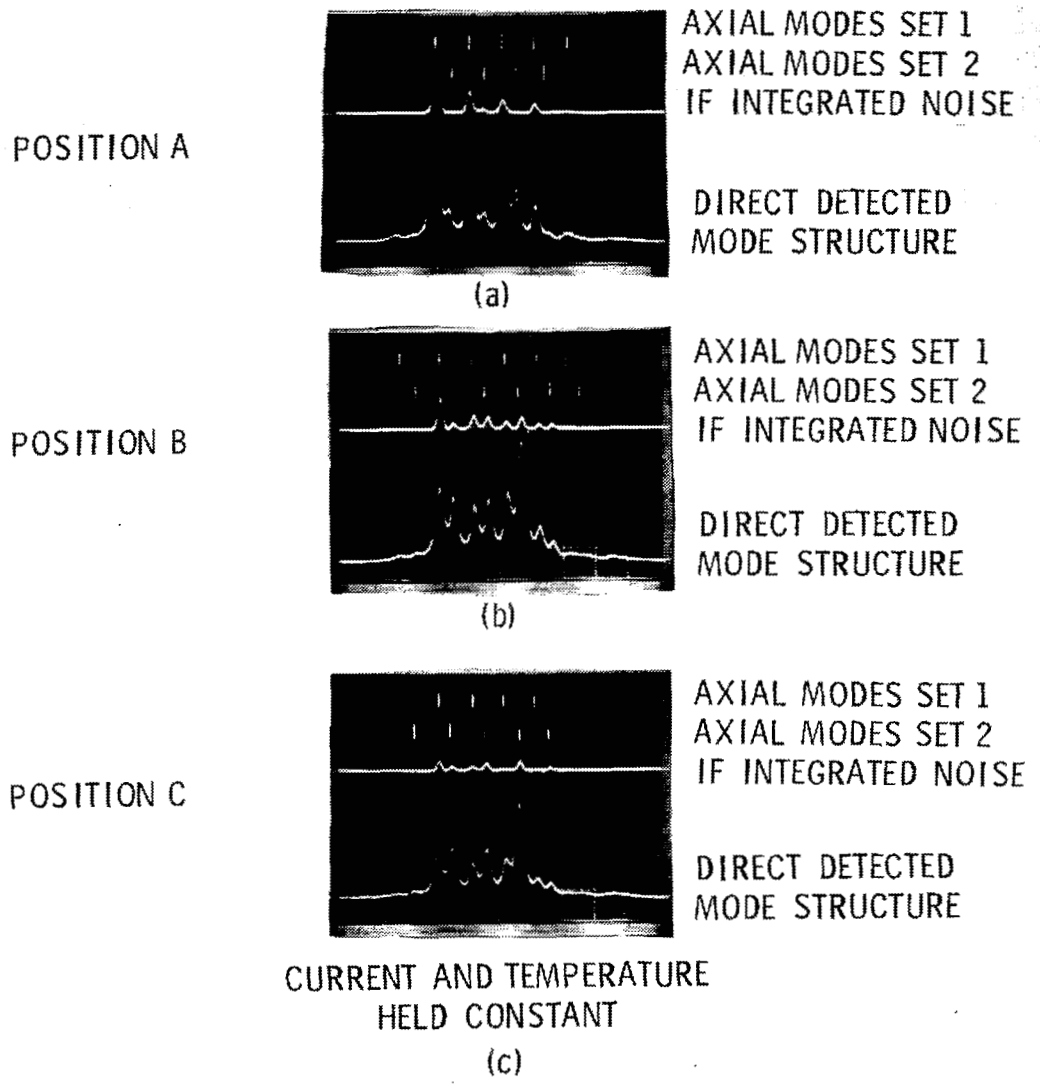

Figure 5.- Spatial dependence of TDL mode power and excess noise.

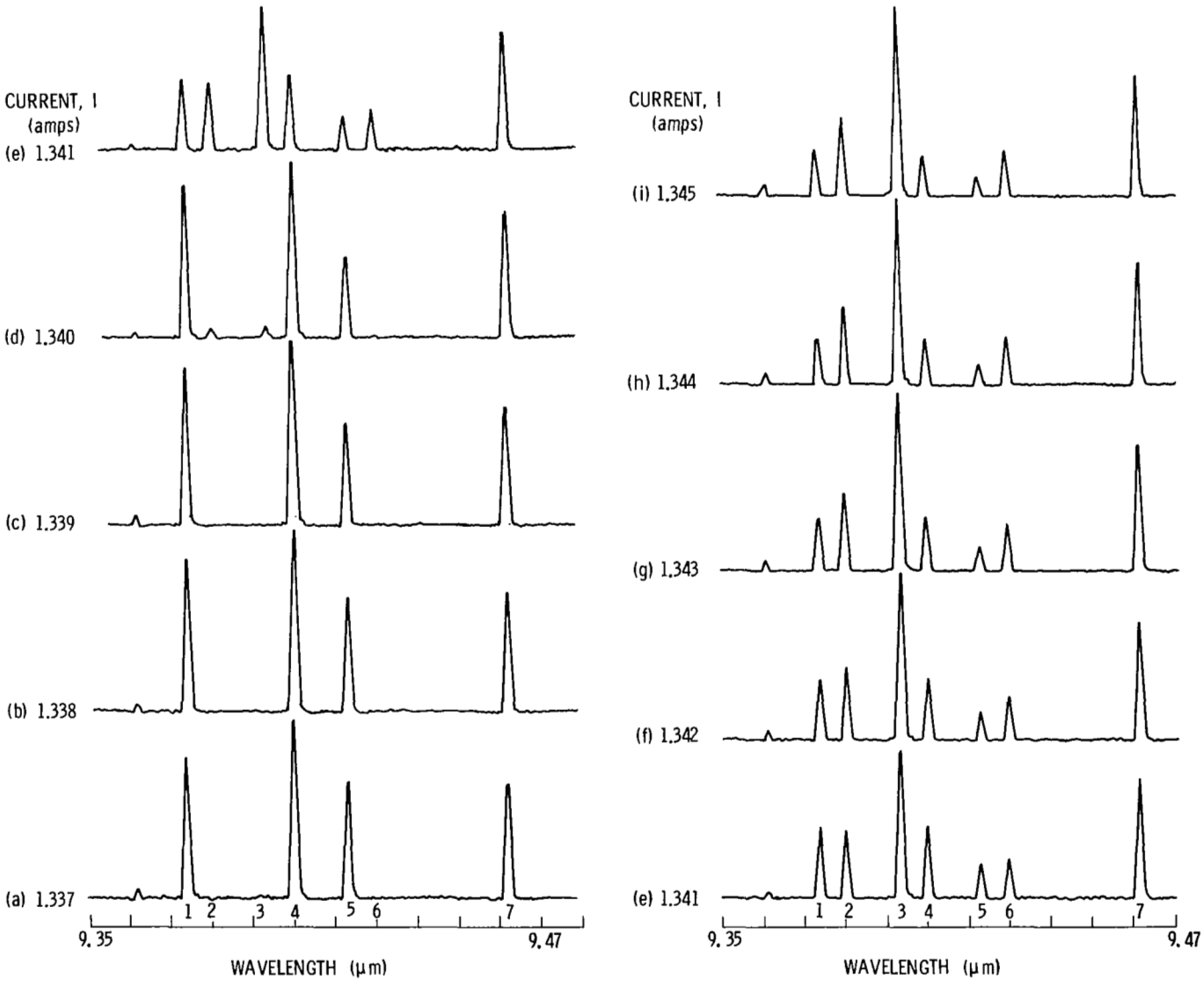

Figure 6.- Current dependence of TDL frequency modes for I = 1.337 to 1.345 amps.

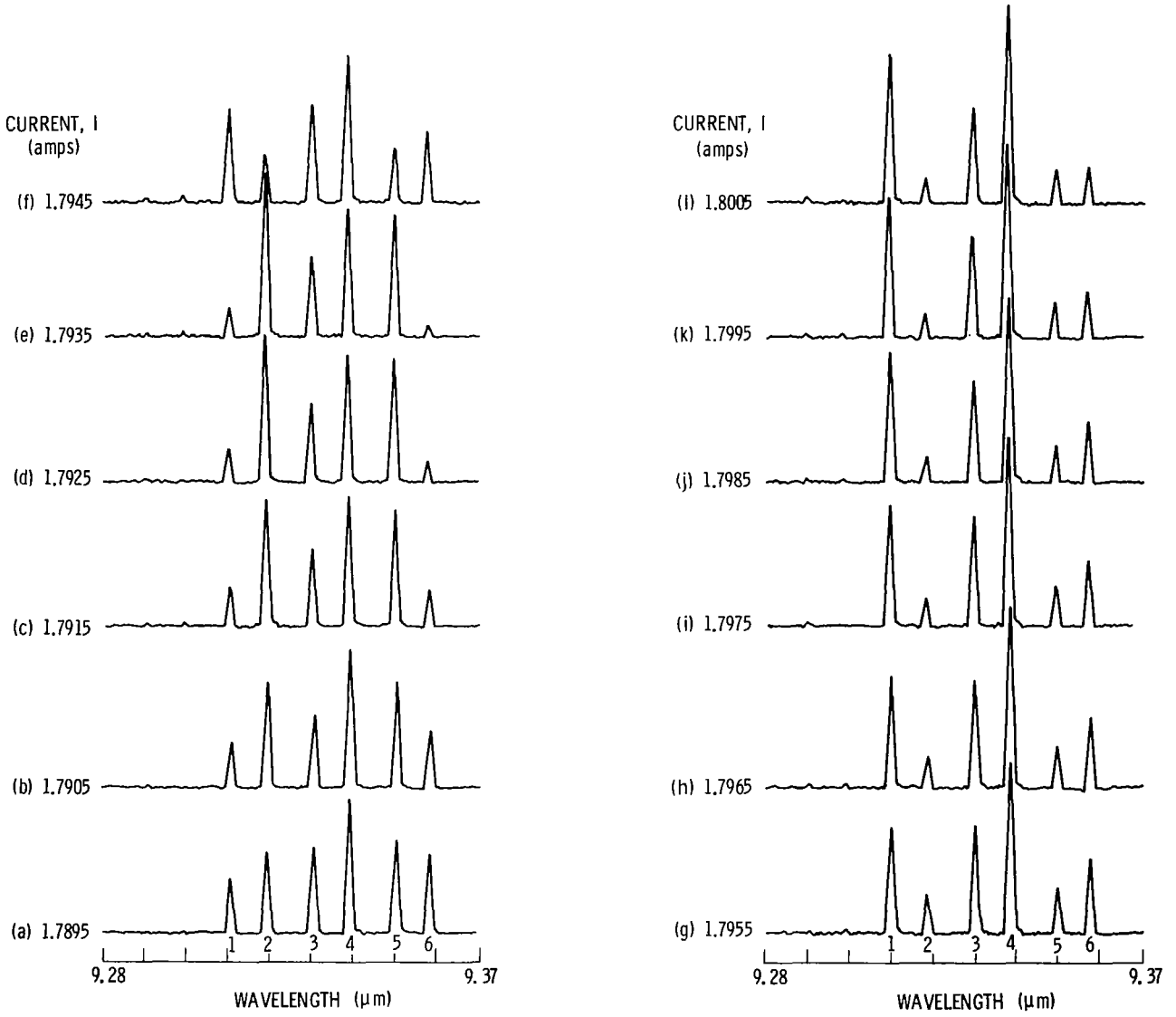

Figure 7.- Current dependence of TDL frequency modes for I = 1.7895 to 1.8005 amps.

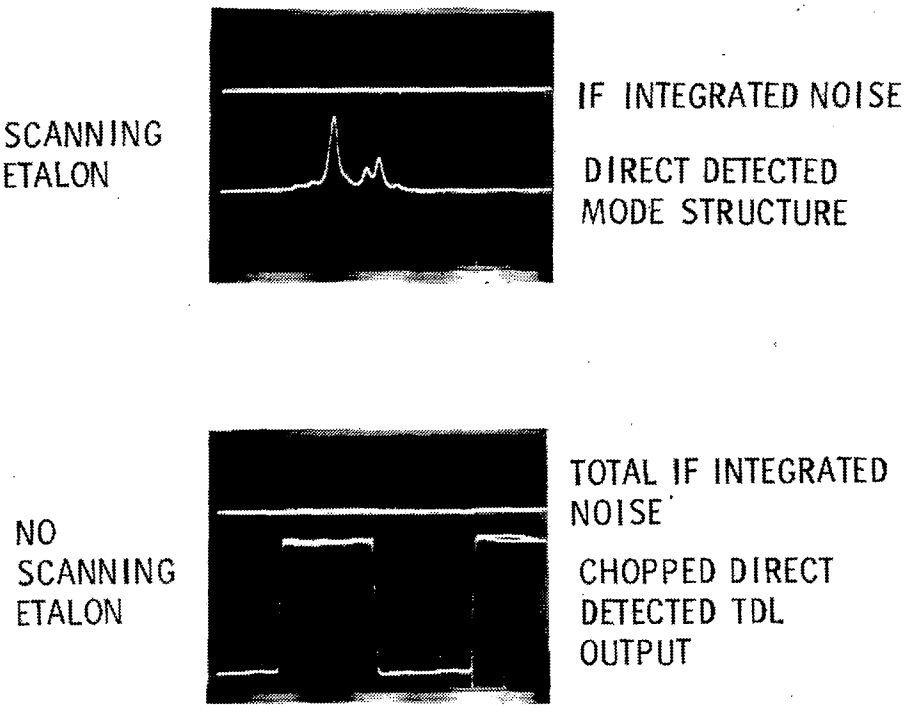

Figure 8.- TDL mode power and total power in absence of excess noise.